Published in final edited form as:
Neuroscience. 2006 October 27; 142(3): 809–822.

Robust Increase of Cutaneous Sensitivity, Cytokine Production and Sympathetic Sprouting in Rats with Localized Inflammatory Irritation of the Spinal Ganglia

Wen-Rui Xie[1,2], **Helen Deng**[3], **Huiqing Li**[1,2], **L. Bowen Travis**[2], **A. Strong Judith**[1], and **Jun-Ming Zhang**[1,2]

1 *Department of Anesthesiology, University of Cincinnati College of Medicine*

2 *Department of Anesthesiology, University of Arkansas for Medical Sciences*

3 *Arkansas Health Department*

Abstract

We investigated the role and mechanisms of inflammatory responses within the dorsal root ganglion (DRG) in the development of chemogenic pathological pain. DRG inflammation was induced by a single deposit of the immune activator zymosan in incomplete Freund's adjuvant in the epidural space near the L5 DRG via a small hole drilled through the transverse process. After a single zymosan injection, rats developed bilateral mechanical hyperalgesia and allodynia which began by day 1 after surgery, peaked at days 3–7, and lasted up to 28 days. The number of macrophages in ipsilateral and contralateral DRGs increased significantly, lasting over 14 days. Robust glial activation was observed in inflamed ganglia. Cytokine profile analysis using a multiplexing protein array system showed that, in normal DRG, all but IL-5, IL-10 and GM-CSF were detectable with concentrations of up to 180 pg/mg protein. Local inflammatory irritation selectively increased IL-1β, IL-6, IL-18, MCP-1, and GRO/KC up to 17 fold, and decreased IL-2 and IL-12 (p70) up to 3 fold. Inflaming the DRG also remarkably increased the incidence of spontaneous activity of A- and C-fibers recorded in the dorsal root. Many of the spontaneously active A-fibers exhibited a short-bursting discharge pattern. Changes in cytokines and spontaneous activity correlated with the time course of pain behaviors, especially light stroke-evoked tactile allodynia. Finally, local inflammation induced extensive sprouting of sympathetic fibers, extending from vascular processes within the inflamed DRG. These results demonstrate the feasibility of inducing chronic localized inflammatory responses in the DRG in the absence of traumatic nerve damage, and highlight the possible contribution of several inflammatory cytokines/chemokines to the generation of spontaneous activity and development and persistence of chemogenic pathologic pain.

Keywords

dorsal root ganglion; inflammation; animal model; low back pain; radiculopathy; spontaneous activity; sympathetic sprouting

Abbreviations used

DRG dorsal root ganglia; ELISA enzyme-linked immunosorbent assay;; GM-CSF granulocyte-macrophage colony stimulating factor; GRO/KC growth related oncogene (also called CXCL1); IFA

Send Correspondence to: Jun-Ming Zhang, M.Sc., M.D., Department of Anesthesiology, University of Cincinnati College of Medicine, 231 Albert Sabin Way, PO BOX 670531, Cincinnati, OH 45267-0531, Tel: 513-558-2427, FAX: 513-558-0995 Email: Jun-Ming.Zhang@uc.edu.

incomplete Freund's adjuvant; IFN interferon-γ; IL interleukin; LID localized inflammation of the DRG; MCP-1 monocyte chemoattractant protein-1 (also called CCL2); POD post-operative day; TNF-α tumor necrosis factor-α; NP nucleus pulposus; GFAP glial fibrillary acidic protein; TH Tyrosine hydroxylase; RM ANOVA Repeated Measures Analysis of Variance

INTRODUCTION

Inflammatory responses in the lumbar dorsal root ganglion (DRG) play key roles in the development of many pathological pain states including chemogenic low back pain and some forms of intractable neuropathic pain. In humans, acute herpes zoster and postherpetic neuralgia result from inflammation in the DRG and along its dermatome following infection or reactivation of the varicella-zoster virus (Schon et al., 1987, Morgan and King, 1998). In laboratory animals, behavioral radiculopathy and sciatica can occur when the DRGs or dorsal roots are inflamed by exposure to material from the nucleus pulposus (NP) (Gertzbein et al., 1977, Kawakami et al., 1996, Olmarker and Myers, 1998, Satoh et al., 1999, Kawaguchi et al., 2001), which is known to possess immunogenic and chemogenic capacities (Gertzbein et al., 1977, Satoh et al., 1999, Kawaguchi et al., 2001).

More recently, it has been recognized that inflammation may also play a role in neuropathic pain (nerve injury) models even though these models do not use inflammation as the primary mechanism of initial injury. For example, inflammatory responses have been demonstrated in DRGs with peripheral nerve injury (Lu and Richardson, 1993, Eckert et al., 1999, Hu and McLachlan, 2002) or injury to the DRG (Zhang et al., 1999). In peripheral nerve injury, macrophages are recruited from blood to the damaged nerve and DRG, where they contribute significantly to the removal of degenerating axons and myelin sheaths, and to regeneration (Beuche and Friede, 1984, Brown et al., 1991, Perry and Brown, 1992, Hu and McLachlan, 2002). In addition, the satellite glia surrounding sensory neuron somata proliferate (Barron et al., 1990, Gehrmann et al., 1991, Lu and Richardson, 1991) and become immunoreactive for glial fibrillary acidic protein (GFAP) (Woodham et al., 1989).

Certain inflammatory cytokines within DRG or injured nerves are known to be associated with pain behaviors (Wagner and Myers, 1996, Sommer et al., 1998a, Sommer et al., 1998b, Ignatowski et al., 1999, George et al., 2000, Svensson et al., 2005). These cytokines play an important role in the development and persistence of nerve injury-induced cutaneous hypersensitivity (DeLeo and Colburn, 1995, Schafers et al., 2003a, Schafers et al., 2003b, Ji and Strichartz, 2004, Watkins and Maier, 2005, Zelenka et al., 2005), and also contribute to the generation of abnormal spontaneous activity from injured nerve fibers (Wagner and Myers, 1996, Sommer et al., 1998a, Sommer et al., 1998b, Ignatowski et al., 1999, George et al., 2000) or compressed DRG neurons (Liu et al., 2002, Zhang et al., 2002, White et al., 2005).

Little is known about how inflammation per se, in the absence of nerve damage, affects the DRG neurons, the cytokine profile within the DRG, and the subsequent animal pain behaviors. Numerous studies have examined inflammation or immune responses as the cause of low back pain/radiculopathy. However, most studies are limited to the acute phase due to the lack of an animal model of chronic epidural or DRG inflammation. Here, using a newly developed animal model of localized inflammation of the DRG (LID), we have examined possible causal factors that mediate pain following DRG inflammation. We characterized changes in cytokine production and their association with development of spontaneous activity as well as with pain and hyperalgesia. This study demonstrates the feasibility of the LID model in addressing neurological mechanisms of low back pain/radiculopathy and other pathologic states that involve inflammatory processes in the DRG.

EXPERIMENTAL PROCEDURES

Animals

Adult, male, Sprague-Dawley rats weighing 200–250 g were housed in groups of 2–4 in 40×60×30 cm plastic cages with soft bedding under a 12/12 h day/night cycle. The rats were kept 7–10 days under these conditions before surgery and up to 4 weeks after surgery. The experimental protocol was approved by the Institutional Animal Care and Use Committees of the University of Cincinnati and University of Arkansas for Medical Sciences.

Localized immune activation by application of zymosan/IFA near the lumbar DRG

Rats were anesthetized by continuous inhalation of isoflurane. On the right side, the paraspinal muscles were separated surgically from the L5-L6 vertebrae. The superior articular process of L6 and the transverse process of L5 vertebrae were cleaned. A small opening (diameter: 0.49 mm) was drilled through the junction of the transverse process and the lamina over the L5 DRG. A 25-G needle was cut short (length: 2–3 mm) and inserted into the opening without contacting the ganglion (Zhang et al., 2001). The needle was connected to a microsyringe loaded with 20 μl zymosan (Sigma) suspended in incomplete Freund's adjuvant (IFA; Sigma) at a concentration of 0.5 μg/μl or 0.05 μg/μl corresponding to total amounts of 10 and 1μg, respectively. The microsyringe was left in place for 2–3 min after injection of the 20 μl zymosan/IFA to prevent solution leakage. Sham-operated rats received the same surgical procedure and injection of 20 μl of oxygenated artificial cerebrospinal fluid (ACSF) containing (in mM): NaCl 130, KCl 3.5, NaH_2PO_4 1.25, $NaHCO_3$ 24, Dextrose 10, $MgCl_2$ 1.2, $CaCl_2$ 1.2 (pH = 7.3). In experiments for cytokine detection and histology, both L4 and L5 DRGs were inflamed by individually depositing equal amount of zymosan (10 μg) in IFA in order to increase the amount of tissue obtained per animal.

Estimation of zymosan spread from injection site

In order to estimate the degree to which the injected zymosan would spread to contralateral and adjacent ganglia, we conducted experiments in 2 rats in which FluoSheres (Invitrogen) sulfate fluorescent microspheres were added to the zymosan/IFA injection solution. Equal volumes of microspheres and zymosan (10μg dose) were added to IFA. The diameter of the microspheres used was 4μm, chosen to be close to the average particle size for the zymosan (yeast cell wall) preparation as reported by the manufacturer (Sigma), and sulfate microspheres were used instead of more hydrophillic types because zymosan is relatively hydrophobic. Examination of whole ganglia mounts on POD5 indicated that fluorescence was distributed throughout the L5 DRG beneath the injection site. No dye spread to the contralateral DRGs was found. Also no dye was observed on the ipsilateral L4 DRG, although some beads appeared on the spinal nerve for the L4 DRG, possibly due to leakage along the region of spinal nerve where the L4 and L5 spinal nerves merge together.

Behavioral testing

Animals were inspected and tested every three days for 10 days prior to surgery, every three days for the first two postoperative weeks, twice during the 3rd week and twice at the end of 4 weeks postoperatively for a total of 12 testing sessions. For general observation, the rats were placed on a table and notes were made on the animal's gait and the posture of each hindpaw and the conditions of the hindpaw nails and skin.

Withdrawal to punctate mechanical stimulation of the foot (mechanical hyperalgesia)—A total of 20 rats were randomly assigned to 3 groups: high dose zymosan/IFA (n = 7), low dose zymosan/IFA (n = 7), and sham control (n = 6). During the behavioral testing, the rat was placed in a clear plastic cage with a floor of plastic wire mesh. The cage

was elevated so that stimuli could be applied to each hind foot from beneath the cage. Von Frey filaments with 100-μm cylindrical tips capable of exerting bending forces of 20, 40, 60, 80, 120 and 160 mN were applied to 6 designated loci on the plantar surface of the foot. The percentage of withdrawal responses was plotted as a function of force; the response threshold was defined as the force corresponding to a 50% withdrawal, as determined by the Hill Equation (Zhang et al., 2000, Homma et al., 2002). The baseline mean withdrawal threshold of each hind paw before surgery was obtained from an average of 3 testing sessions, 1 session every 3 days (plotted as day 0). For each postoperative testing session, difference scores were computed by subtracting the baseline withdrawal threshold from each postoperative day threshold. Negative scores indicate a decreased threshold after surgery.

Withdrawal to light stroke of the foot (tactile allodynia)—A total of 19 rats, 12 zymosan-treated, and 7 sham control, were tested for foot withdrawal to innocuous tactile stimulation before and after surgery. A wisp of cotton pulled up from, but still attached to a cotton swab was stroked mediolaterally across the plantar surface of the skin through the floor of the plastic cage. Six strokes were delivered to each hind paw, alternating between right and left with each stroke. A single quick withdrawal reflex was considered to indicate the existence of tactile allodynia. The incidence of withdrawals was expressed as a percentage of the six strokes for each foot. The stimulus was defined as normally innocuous because control rats never exhibited a withdrawal response.

Thermal pain testing—In preliminary experiments, sensitivity of the paw to a thermal heat stimulus was examined up to POD 17 using the method of Hargreaves et al. (Hargreaves et al., 1988). These experiments showed that zymosan/IFA treatment resulted in only very small increases in thermal sensitivity (n = 6). The largest changes were observed on day 11, when the withdrawal threshold fell from a baseline value of 9.6 ± 0.4 seconds to 8.2 ± 0.3 seconds ($p = 0.1$, Student's t-test) on the ipsilateral side, and from 10.2 ± 0.9 seconds to 8.3 ± 0.2 seconds ($p = 0.02$, Student's t-test) on the contralateral side. Repeated measures ANOVA did not reveal significant changes in thermal sensitivity from baseline on any of the postoperative days tested (up to POD 17). For comparison, we observed thermal sensitivity decreases of 3 to 5 seconds, from a similar baseline value, in our previous study using the CCI and SNI pain models (Xie et al., 2005). Because thermal pain sensitivity changes were small and nonsignificant, we focused on mechanical pain sensitivity for the rest of this study.

Immunostaining of activated macrophages and GFAP-positive glia in the DRG

A 10-μm frozen section was cut from the harvested DRG every 30 μm, picked up on polylysine coated slides, and allowed to air-dry overnight. Sections were first incubated with rat-absorbed mouse anti-rat ED-2 (1:1,000) (Serotec, Inc., Raleigh, NC), a specific marker for macrophages, or rabbit anti-rat GFAP (1:800) (Immunostar, Hudson, WI), a marker for activated glia, overnight at room temperature followed by a reaction with horse anti-mouse and goat anti-rabbit biotinylated secondary antibodies, respectively (Vector Laboratories, Burlingame, CA). The immunoreactive products were visualized using the diaminobenzidine (DAB) method for ED-2 and DAB or Alexa Fluor 594 fluorescent dye (Invitrogen Corp., Carlsbad, CA) for GFAP.

Using ImagePro Plus software (Media Cybernetics, Inc., Silver Spring, MD), non-overlapping, adjacent images from each section were digitized under a light microscope equipped with a color digital camera and stored in a computer. To estimate the density of macrophages, positively stained macrophage profiles were counted and then normalized by the number of neurons in the analyzed image area to give a density ratio (number per neuron).

Profiling of cytokines in normal and inflamed DRG

Cytokine expression profiles in the normal and inflamed DRG were evaluated using Bio-Plex System (Bio-Rad, Hercules, CA, USA) combined with Linco 14-Plex Rat Cytokine Detection Kit. A total of 14 rat cytokines were measured simultaneously from a single well according to the manufacturer's protocols. Briefly, normal, sham, or inflamed ipsilateral DRGs (L4 and L5) were isolated from the rats on postoperative days (POD) 1, 3, 7, 14, 21, and 28. Tissue was homogenized (3 pulses, 15 sec each with a 3 min interval between pulses) using a PowerGen 125 at 4C° in lysis buffer (Bio-Rad, Hercules, San Diego, CA) supplemented with a protease inhibitor cocktail (Sigma, St. Louis, MO) followed by centrifugation (13,000 rpm) at 4°C for 30 min to obtain extracted protein.

The cytokine detection kit contains color-coded microspheres conjugated with a monoclonal antibody specific for a target protein. Protein samples (25 μl) extracted from DRG tissue were thawed and run in duplicate. Antibody-coupled beads were incubated with the tissue sample (antigen) after which they were incubated with biotinylated detection antibody before finally being incubated with streptavidinphycoerythrin. A broad sensitivity range of standards (Linco Research, Inc. MI, USA) ranging from 4.88 to 20,000 pg/ml was used to allow the quantization of a dynamic wide range of cytokine concentrations and provide the greatest sensitivity. This captured immunoassay was then read by the Bio-Plex System which uses Luminex fluorescent-bead-based technology (Luminex Corporation Austin, TX, USA) with a flow-based dual laser detector with real-time digital signal processing to detect both the color code and the signal intensity of each bead, allowing simultaneous quantification of multiple proteins in a single sample. This method was chosen because it has sensitivity and performance similar to ELISA methods, but requires much smaller sample volumes and is suitable for mutiplexing (duPont et al., 2005).

The concentrations of cytokines in these assays were calculated using a standard curve. A regression analysis was performed to derive an equation that was then used to predict the concentration of the unknown samples. The measured cytokines were interleukin-1α (IL-1α), IL-1β, IL-2, IL-4, IL-5, IL-6, IL-10, IL-12 (p70), IL-18, interferon-γ (IFN), tumor necrosis factor-α (TNF-α), granulocyte-macrophage colony stimulating factor (GM-CSF), growth related oncogene (GRO/KC) and monocyte chemoattractant protein-1 (MCP-1).

The final concentrations of the 14 cytokines were obtained from an average of values observed in 3 to 5 samples for each time point and condition. Each individual sample contained 4 DRGs combined from 2 rats, measured in duplicate. Data were normalized to the amount of protein and to the tissue weight, as indicated.

In vitro microfilament recording and determination of the incidence of spontaneous activity

As described in our earlier publication (Zhang et al., 1997), under general anesthesia, a laminectomy was performed at the L3–L6 level, and the L_5 DRG with attached sciatic nerve and dorsal root was mounted in a recording chamber after being removed from the rat. The DRG was secured by fine pins to the Sylgard base in the central chamber (5 mm in diameter). The dorsal root was led from this chamber and into an adjacent chamber (filled with mineral oil), where microfilament recordings were performed. The sciatic nerve was covered with Vaseline, and a bipolar-stimulating electrode was used for electrical stimulation. The DRG was continuously perfused at a rate of 5 ml/min with ACSF. The temperature was kept at 37° ± 0.5°C by running the perfusing solution through a temperature-controlled inline heater (Warner Instruments Corporation, Hamden, CT). Electrical activity was recorded extracellularly via laboratory interface and computer acquisition software (Spike2, Cambridge Electronic Design, Inc, England). Nerve fibers were classified as C- (<1.5 m/s), Aδ- (1.5–15 m/s), or Aβ-fibers (>15 m/s) based on the conduction velocity of impulses evoked by electrical

stimulation of the nerve. The Govrin-Lippmann and Devor method (Govrin-Lippmann and Devor, 1978) was used to measure the incidence of ongoing discharge in those fibers where conduction velocity could be measured by electrical stimulation of the sciatic nerve. For each fiber bundle of approximately equal diameter (≈40–50 μm), the sciatic nerve was stimulated with a gradually increasing intensity of current (0.1–0.5 ms square wave pulses, 1–2 Hz) up to 10 mA, resulting in a gradual recruitment of dorsal root fibers until the number of fibers saturated. The total number of different action potential waveforms was counted and summed for all strands and divided by the total number of fibers (in all strands) recruited by electrical stimulation of the sciatic nerve to obtain the incidence of ectopic discharge.

Tyrosine hydroxylase (TH) immunostaining of sympathetic fibers

Tissue sections (40 μm) were cut using a Vibratome (St. Louis, MO) and incubated in antibodies to tyrosine hydroxylase (TH) (raised from rabbit; obtained from Pel-Freeze, Rogers, AR) at a dilution of 1:1,000 for 48 hours at 4 °C, followed by reaction with biotinylated secondary antibody and, finally, with Vector ABC reagent. Triton-X (0.3%) was used in all reaction solutions to enhance antibody penetration. Immunoreaction products were visualized by the DAB method in the presence of H_2O_2 in 0.1 M phosphate buffer. Tissues were then mounted on gelatin-coated slides, air dried, dehydrated, and coverslipped for light-microscopic observation.

Data analysis

Data are expressed as means and standard errors of the mean. Differences in withdrawal thresholds over time were tested using one-way Repeated Measures Analysis of Variance (RM ANOVA) followed by all pairwise posthoc comparisons (Tukey method). Difference in withdrawal thresholds between groups (e.g., high dose vs. low dose) was tested using two-way RM ANOVA. Cytokine concentrations below the detection level of the experiment were assigned a value of zero for purposes of calculating average concentrations. Differences in macrophage densities between groups were compared using Student's t-test. $P<0.05$ was chosen as the criterion for significance.

RESULTS

General observations

All animals appeared in good health throughout the testing period. The level of general activity was normal before and after surgery. Their fur was sleek and well groomed. No changes in gait or posture were observed in any rats of the sham or zymosan groups before or after surgery. There were no signs to indicate that rats were trying to reduce the weight placed upon the ipsilateral paw by leaning to the other side or by sitting on the opposite haunch as observed in other rodent models of pathological pain. However, when a mechanical or thermal stimulus was applied to the hind paws during postoperative testing, the reflex withdrawals were of great amplitude and excessive duration during which the paw was held in the air typically 2 – 15s. At times, a withdrawal of the hind paws was accompanied by exaggerated aversive behavior such as licking the stimulated paw. When the same stimuli were applied to the hind paw during preoperative testing, the reflex withdrawals were brief and of smaller amplitude.

Localized epidural inflammation near the L5 DRG unilaterally induced prolonged bilateral mechanical hyperalgesia and tactile allodynia

Local application of zymosan/IFA induced bilateral hyperalgesia for up to 28 days post-operatively. Ipsilateral withdrawal thresholds dropped significantly on the first postoperative day for both high (10 μg, n=7) and low (1μg, n=7) doses of zymosan. Withdrawal thresholds steadily decreased until reaching a minimum threshold on POD 3 ($p<0.05$, One-way RM

ANOVA). Threshold levels then began to steadily approach, but never returned to, pre-operative levels over the next 3 weeks. A higher dose of zymosan substantially decreased the withdrawal threshold when compared to the lower dose zymosan or the sham control (Figure 1A, B) ($p<0.05$, two-way RM ANOVA).

Local zymosan/IFA application on the DRG also induced an increased sensitivity in the contralateral foot, albeit with a slower onset. As was the case for the ipsilateral side, thresholds steadily approached, but never met, pre-operative levels through POD 28. Rats receiving buffered saline injection showed a slight, bilateral decrease in withdrawal threshold, which quickly returned to pre-surgical level before POD 7 (Figure 1C).

Prior to surgery, none of the 12 rats in the zymosan group (10 μg) exhibited any reflex withdrawals to light strokes of either foot with the cotton wisp. On the first postoperative day, however, light strokes of the ipsilateral or contralateral foot evoked a reflex withdrawal to at least one of the 6 strokes (tactile allodynia). The incidence of foot withdrawal to stroking was higher for the ipsilateral than the contralateral foot. The incidence of light stroke-evoked reflexes peaked on POD 3 and decreased during subsequent testing. By POD 14, none of the rats withdrew to the stimulus applied to either foot (Figure 1D). None of the 7 ACSF-treated sham rats exhibited any quick withdrawal response to light strokes with the cotton wisp during the entire 28-day testing period (data not shown).

Macrophage response and glial activation in the inflamed DRG

Depositing zymosan (10 μg) in IFA on the L5 DRG resulted in prolonged macrophage response in the DRG (Figure 2). Ipsilaterally the macrophage density ratio (# of macrophage per neuron) peaked at POD 7, increasing to 0.78, nearly four times that of normal DRGs and more than triple that of the saline control (Figure 2, Figure 3, top panel). Density ratios remained considerably above normal while decreasing after POD7 with a POD 14 density ratio of 0.6; which was still nearly double the density of normal DRGs. Contralateral values increased more gradually with a POD 2 density ratio of 0.3 and a peak density ratio of 0.4 at POD 14 (Figure 3, bottom panel). Macrophage responses were also observed in DRG treated with low dose zymosan (1 μg). Macrophages were diffusely located throughout the inflamed DRG.

As shown in Figure 4, incubation of inflamed DRG sections, yielded strong rings (activated satellite glia) of signal around almost all of the large, medium and small-sized neurons that intensified with time within the first 2 postoperative weeks followed by a slow recovery but never returned completely to the presurgical level by 3 weeks postoperatively (Figure 4A, B). GFAP-positive rings were also observed in some areas of the contralateral DRG sections (Figure 4C). However, incubating normal DRG sections with the anti-GFAP antibody yielded little to no signal (Figure 4D).

Selective up- and down-regulation of cytokines in the inflamed DRGs as measured by multiplexing technology

As shown in Table 1, in normal DRG, of the 14 cytokines examined, all but IL-5, IL-10, and GM-CSF were detectable. Local zymosan/IFA application (10 μg) remarkably increased IL-1β, IL-6, IL-18, MCP-1, and GRO/KC up to 17 fold with much larger increases in zymosan-treated animals than in sham animals (Figure 5). Levels of IL-2 and IL-12 (p70), decreased by up to 3 fold although decreases of similar magnitude were also observed in sham operated animals (Figure 6). Levels of IL-1α, TNF-α and IFN were not strongly or consistently affected by localized inflammatory irritation. Levels of IL-4 seemed to decrease, in that a larger fraction of samples had concentrations below the detection level, but because the levels even in normal rats were close to the detection limit, quantification of decreased levels could not be obtained, and differences between sham and zymosan treated rats were not clearly evident.

As shown in figure 5, the largest changes in cytokine levels were observed on days 1 and 3. Most cytokines that had increased, declined back towards control levels considerably by day 7, though some still remained above control levels. An exception was IL-18, which showed similar increases through day 21. The two cytokines (IL-12 and IL-2) for which we were able to measure zymosan/IFA-induced decreases also showed changes that lasted through day 21.

Generation of spontaneous activity in the inflamed DRG

Spontaneous (ectopic) activity, thought to be an important correlate of pathological pain in many chronic pain models (Wall et al., 1979, Burchiel, 1984, Devor et al., 1992, Xie et al., 2005), was examined in normal ganglia and those inflamed with zymosan (10 μg) in IFA. As summarized in Table 2, C-fibers were recorded from inflamed DRG via electrical stimulation of the sciatic nerve on POD 3, 7 and 14. Of the C-fibers, 4 to 11% were spontaneously active with the highest and only significantly different percentage observed on POD 3. All of the spontaneously active C-fibers recorded exhibited discharges with irregular interspike intervals and a low frequency that was typically 0.5 to 1 Hz. Spontaneous activity was also recorded from 5 to 9% of Aδ-fibers in inflamed ganglia, however, these increases did not reach statistical significance. The highest incidence of spontaneous activity was observed in Aβ-fibers, 10 to 16 % of which exhibited ectopic spontaneous activity within the inflamed DRG.

Thirty-two percent of the spontaneously active Aβ-fibers had a bursting pattern (Figure 7). The number of spikes within a single burst was 2 to 7 spikes per burst in the majority of these fibers (82% fell within this range on day 3, falling to 63% on day 7 ($p<0.0001$ vs. day 3), and to 59% on day 14), though a minority of fibers had much larger values of 10 – 40 spikes per burst, bringing the average number of spikes per burst up to 6.7 ± 1.3 on day 3. On days 7 and 14 a small number of fibers (6 – 12 %) displayed ultra long bursts of over 100 spikes. The interspike interval within each burst decreased from 39.6 ± 1.6 msec on day 3 to 26.8 ± 3.9 msec on day 14 ($p < 0.01$), with an intermediate value on day 7.

The patterns of the remaining spontaneously active, nonbursting fibers were either irregular or regular firing without bursting. Fibers with high-frequency (>15 Hz), irregular discharges were rare. The incidence of spontaneous activity was also measured for 4 unoperated normal rats. As previously observed in our lab (Zhang et al., 2002), the incidence of spontaneous activity was quite low (Table 2).

Sympathetic sprouting in the inflamed DRGs

In 6 zymosan-treated rats (10 μg), the ipsilateral DRGs were dissected on POD 3 (n=2), 7 (n=2) or 14 (n=2) for immunohistochemical staining of the sympathetic fibers. In our previous studies, we have found that in normal DRGs, “dark cells” with TH-IR “tails” were scattered throughout the sections. TH-positive sympathetic fibers were rare. No abnormal growth of the sympathetic fibers was found in any sections from any vascular process (Zhang et al., 2004). In the inflamed DRGs, however, robust sprouting of the sympathetic fibers was observed in all sections beginning as early as day 3 after surgery. It was shown clearly in most sections that the sprouted fibers originated from the vascular processes (Figure 8A, B). The level of sprouting further increased on day 7 and persisted on day 14. As in axotomized DRGs, the sprouted fibers sometime formed basket-like structures around large- and medium-sized DRG neurons (Figure 8C, D).

DISCUSSION

Mechanical deformation and/or inflammatory irritation of the DRG and its nerve roots is a possible consequence of certain disorders, such as spinal stenosis, disk herniation, spinal injury, or tumors (Hoch et al., 1993, Sato and Kikuchi, 1993, Briggs and Chandraraj, 1995, Poletti,

1996). Clinical studies indicate that inflammation in the vicinity of the DRG may occur with or without apparent anatomic abnormalities. The mechanisms underlying inflammatory responses in the DRG and resultant low back pain and painful radiculopathy may be different in compressive vs. non-compressive injuries. In our previous studies, we have found that mechanical compression of the DRG by insertion of a metal rod into the intervertebral foramen induces pain and hyperalgesia by enhancing sensory neuron excitability (Song et al., 1997, Zhang et al., 1999) and possibly by causing synthesis and release of inflammatory cytokines within the compressed DRG (Homma et al., 2002). In the present study, we have created a new animal model, which will allow us to study inflammation, independently from compression or injury, as a biological factor contributing to the development of radiculopathy and sciatica. It was found that pain and hyperalgesia occurred in all rats after an injection of a small amount (1 to 10 μg) of the immune activator zymosan in IFA over one L5 DRG. The mechanical threshold to evoke a painful withdrawal response dropped to the lowest level within a week and remained low during the first two weeks. The tactile allodynia evidenced by painful foot withdrawal to light strokes using a piece of cotton wisp was present in all rats for the first two weeks. Although light stroke was not able to evoke withdrawal responses after POD14, cutaneous sensitivity remained higher than pre-surgical levels through the rest of our testing period. The time course of these pain behaviors correlated with the inflammatory responses in the DRGs as indicated by elevated numbers of macrophages and satellite glia between day 1 and day 14. In preliminary experiments, we found that inflaming the L5 DRG did not alter the withdrawal thresholds of the ipsilateral or contralateral hind paws to thermal stimulation. Thus, in the present study, we have focused on changes in mechanical sensitivity.

The rat cytokine protein array used in the present study can simultaneously detect 14 different cytokines with high specificity and sensitivity, comparable to that obtained with ELISA (duPont et al., 2005). This is the first protein level, cytokine profiling of the DRGs. It shows that in normal DRGs most cytokines are detectable. Zymosan/IFA treatment significantly altered cytokine levels. Consistent elevations, well above the levels seen in sham-operated animals, were observed for IL-1β, IL-6, IL-18, MCP-1, and GRO/KC, cyokines that are traditionally classified as pro-inflammatory based on their effects on classical immune cells; in contrast, anti-inflammatory cytokines IL-2 and IL-12 declined.

In the main these results are consistent with those seen in DRG in some other pain models. Pro-inflammatory cytokines are often elevated in pain states (as well as in other pathologies of the nervous system) and often have anti-analgesic roles though this can not be uniformly assumed (Watkins and Maier, 2002). However, these cytokines may also play protective roles in nervous system pathologies, and it is not yet clear how findings on the neuroprotective roles of pro-inflammatory cytokines in the CNS (Stoll et al., 2000, Felderhoff-Mueser et al., 2005) will apply to pathological pain, in which abnormal neuronal activity rather than neuronal death may play a more important role. Some of the elevated cytokines we observed, namely IL-1β, IL-6, and MCP-1, have previously been found in DRG in many studies; their receptors shown to be present on neurons and/or satellite glia; and their levels increased in various pain models. Several lines of evidence indicate the importance of these cytokines in mediating chronic pain states: i.t. and peripheral application of these cytokines can induce or enhance pain states; genetically modified mice lacking particular cytokines or their receptors have reduced pain in various models; and these cytokines have acute and long-term excitatory effects on DRG neurons (including nociceptors), and can enhance release of pain neurotransmitters (for review, see Watkins and Maier, 2002, Sommer and Kress, 2004).

One relatively new finding in our cytokine profile is the large increase in GRO/KC (also called CXCL1) in LID. There are few previous studies on the role of this cytokine in DRG, though it has been shown to enhance peptide release from neonatal DRG nociceptors in vitro and to induce hyperalgesia after peripheral injection (Qin et al., 2005). However, GRO/KC has been

implicated in several CNS pathologies (e.g., Xia and Hyman, 2002, Losy et al., 2005, Valles et al., 2006), and can acutely modulate activity of cerebella neurons (Giovannelli et al., 1998). Similarly, there are few studies on the role of IL-18 in DRG, though it has been extensively studied in models of various CNS pathologies (Felderhoff-Mueser et al., 2005). In our study, IL-18 was notable for the more prolonged time course of its elevation.

Another interesting result of our cytokine measurements was that we found no consistent increases in TNF-α level in the inflamed DRG. In fact, the level on day 3, near the peak of pain behavior effects, we observed a small decrease (Table 1). This change was confirmed using a different cytokine assay kit from Bio-Rad (data not presented here). In our previous study (Homma et al., 2002), we found that perfusion of the compressed DRG with soluble TNF-α receptors led to a very small, albeit significant, decrease in pain behaviors. Thus, our data suggest that TNF-α plays only a minor role in the pain induced by the DRG compression or localized inflammation (e.g., LID). This contrasts with the extensive evidence for a role of TNF-α in peripheral nerve injury and peripheral inflammation models. These results highlight the importance of examining a number of different cytokines, now that this has become technically feasible.

The sources of cytokines in the inflamed DRG are not yet known. Activated satellite glia and macrophages are known to produce a number of cytokines in the early phases of inflammatory process and thus could contribute to the increased cytokine levels in the inflamed DRG. The slower time course of glial activation and macrophage infiltration compared with pain behaviors and changes in cytokine levels in the inflamed DRG might suggest that glia or macrophages are not likely to be the major sources of the elevated cytokines or a major cause of the pain behaviors. However, this interpretation is limited by the fact that these cells might rapidly release cytokines such as IL-1β, IL-18, IL-6, and TNF-α by converting them from the pre-existing pools of the inactive forms into the active, releasable forms – such a release might occur much more rapidly than upregulation of glial activation marker proteins that we measured, and in addition would presumably not be detected by our antibody-based detection system. Certain cytokines/chemokines such as MCP-1 and IL-1β can be synthesized and released from the sensory neurons in the DRG (Copray et al., 2001, White et al., 2005). Another possible source of chemotactic cytokines is the endothelial cells which can be activated by pro-inflammatory cytokines (Martiney et al., 1998).

The incidence of spontaneous activity in dorsal root fibers was high on POD 3–7 and dramatically decreased to a lower level by POD14. The time course for myelinated A-fibers (e.g., Aδ- and Aβ-) correlated well with the inflammatory response as well as the development of painful behaviors. In a recent in vitro study, it was found that topical DRG application of an inflammatory cocktail consisting of histamine, prostaglandins E2 (PGE_2), serotonin (5-HT), and bradykinin robustly enhanced the excitability of the sensory neurons with intact or injured peripheral axons (Song et al., 2003). In another study, MCP-1 was found to excite chronically compressed DRG neurons in vitro (White et al., 2005). These results and results from our current study have led us to hypothesize that the initiation or development of abnormal spontaneous activity from inflamed DRG neurons may be attributed to the increased cytokine production and possibly to resultant elevated levels of inflammatory mediators within the DRG. The incidence of spontaneous activity with a bursting pattern is significantly higher shortly after surgery, especially the short-burst discharges. Similar observations were made in chronically compressed DRGs (Song et al., 1999). This suggests that in compressed DRGs, the bursting discharges may be caused by intraganglionic inflammation.

Sympathetic sprouting occurred in all inflamed DRGs beginning as early as day 3 of surgery. It can be clearly observed that sprouted fibers originate from the vascular processes in the DRGs. Fiber sprouting may be explained by increased expression of certain inflammatory

cytokines such as IL-6, which has been reported to be able to cause sympathetic growth (Ramer et al., 1998, Ramer et al., 1999). Other factors such as NGF and NT-3 may be involved, too (Zhou et al., 1999). Results of this study indicate that sympathetic sprouting may occur in intact DRG without peripheral axotomy. Extensive sympathetic sprouting in the inflamed DRG suggests a possible sympathetic component in this model as reported in other inflammatory pain conditions (Nakamura and Ferreira, 1987).

It is of interest to compare the LID model with the previously described sciatic inflammatory neuritis (SIN) model of Chacur at al. (2001) in which pain was induced by injecting zymosan around the sciatic nerve. Both models produce mechanical but not thermal pain behaviors. SIN is associated with localized increases in IL-1β, as we observed in LID, but also results in increased TNF-α release. Both models produce both contralateral and ipsilateral pain at higher zymosan doses. Milligan et al. suggested that this phenomenon was possibly mediated by glial activation across the spinal cord. They found that the bilateral allodynia induced by SIN can be prevented or reversed by intrathecal application of glial inhibitors, inhibitors of p38 mitogen-activated kinases, or proinflammatory cytokine antagonists specific for interleukin-1, TNF-α, or interleukin-6 (Milligan et al., 2003). Contralateral allodynia and hyperalgesia in rats with zymosan/IFA treatment of a single DRG may share similar mechanisms. The possibility of zymosan diffusion in contributing to the development of contralateral allodynia cannot be completely ruled out, though our experiments with fluorescently labeled microspheres argue against this possibility.

Evidence for spinal contributions to pain induced by DRG inflammation was also obtained in another study, in which topical application of autologous NP to the L5 DRG remarkably increased the sensitivity of WDR neurons in response to mechanical or thermal stimulation of the peripheral receptive fields (Cuellara et al., 2004). Both NP and zymosan/IFA are considered to be immune activators and thus may share similar peripheral and spinal mechanisms in causing pain and hyperalgesia.

In summary, the current study demonstrated that localized immune activation in the vicinity of the L5 DRG induced prolonged inflammatory responses and elevated cytokine production along with enhanced spontaneous activity of DRG neurons and subsequent development of bilateral allodynia in the rats. These results have demonstrated a promising animal model for the study of neurological mechanisms of chemogenic low back pain, radiculopathy and sciatica, which may also become a reliable tool for the development and assessment of new therapies targeting these types of pathological conditions.

Supplementary Material

Refer to Web version on PubMed Central for supplementary material.

Acknowledgements

This work was supported in part by NIH grants NS39568 and NS45594 (J.Z.).

References

Barron KD, Marciano FF, Amundson R, Mankes R. Perineuronal glial responses after axotomy of central and peripheral axons. A comparison. Brain Res 1990;523:219–229. [PubMed: 1698104]

Beuche W, Friede RL. The role of non-resident cells in Wallerian degeneration. Journal of Neurocytology 1984;13:767–796. [PubMed: 6512566]

Briggs CA, Chandraraj S. Variations in the lumbosacral ligament and associated changes in the lumbosacral region resulting in compression of the fifth dorsal root ganglion and spinal nerve. Clin Anat 1995;8:339–346. [PubMed: 8535966]

Brown MC, Perry VH, Lunn ER, Gordon S, Heumann R. Macrophage dependence of peripheral sensory nerve regeneration: possible involvement of nerve growth factor. Neuron 1991;6:359–370. [PubMed: 1848079]

Burchiel KJ. Spontaneous impulse generation in normal and denervated dorsal root ganglia: sensitivity to alpha-adrenergic stimulation and hypoxia. Exp Neurol 1984;85:257–272. [PubMed: 6745375]

Chacur M, Milligan ED, Gazda LS, Armstrong C, Wang H, Tracey KJ, Maier SF, Watkins LR. A new model of sciatic inflammatory neuritis (SIN): induction of unilateral and bilateral mechanical allodynia following acute unilateral peri-sciatic immune activation in rats. Pain 2001;94:231–244. [PubMed: 11731060]

Copray JC, Mantingh I, Brouwer N, Biber K, Kust BM, Liem RS, Huitinga I, Tilders FJ, Van Dam AM, Boddeke HW. Expression of interleukin-1 beta in rat dorsal root ganglia. J Neuroimmunol 2001;118:203–211. [PubMed: 11498255]

Cuellara JM, Montesanob PX, Carstens E. Role of TNF-alpha in sensitization of nociceptive dorsal horn neurons induced by application of nucleus pulposus to L5 dorsal root ganglion in rats. Pain 2004;110:578–587. [PubMed: 15288398]

DeLeo, JA.; Colburn, RW. The role of cytokines in nociception and chronic pain. In: Weinstein, JN.; Gordon, SL., editors. Low Back Pain: A scientific and clinical overview. American Academy of Orthopaedic Surgeons; 1995. p. 163-185.

Devor M, Wall PD, Catalan N. Systemic lidocaine silences ectopic neuroma and DRG discharge without blocking nerve conduction. Pain 1992;48:261–268. [PubMed: 1589245]

duPont NC, Wang K, Wadhwa PD, Culhane JF, Nelson EL. Validation and comparison of luminex multiplex cytokine analysis kits with ELISA: determinations of a panel of nine cytokines in clinical sample culture supernatants. J Reprod Immunol 2005;66:175–191. [PubMed: 16029895]

Eckert A, Segond von Banchet G, Sopper S, Petersen M. Spatio-temporal pattern of induction of bradykinin receptors and inflammation in rat dorsal root ganglia after unilateral nerve ligation. Pain 1999;83:487–497. [PubMed: 10568857]

Felderhoff-Mueser U, Schmidt OI, Oberholzer A, Buhrer C, Stahel PF. IL-18: a key player in neuroinflammation and neurodegeneration? Trends Neurosci 2005;28:487–493. [PubMed: 16023742]

Gehrmann J, Monaco S, Kreutzberg GW. Spinal cord microglial cells and DRG satellite cells rapidly respond to transection of the rat sciatic nerve. Restorative Neurology & Neuroscience 1991;2:181–198.

George A, Marziniak M, Schafers M, Toyka KV, Sommer C. Thalidomide treatment in chronic constrictive neuropathy decreases endoneurial tumor necrosis factor-alpha, increases interleukin-10 and has long-term effects on spinal cord dorsal horn met-enkephalin. Pain 2000;88:267–275. [PubMed: 11068114]

Gertzbein SD, Tait JH, Devlin SR. The stimulation of lymphocytes by nucleus pulposus in patients with degenerative disk disease of the lumbar spine. Clinical Orthopaedics & Related Research 1977:149–154. [PubMed: 852173]

Giovannelli A, Limatola C, Ragozzino D, Mileo AM, Ruggieri A, Ciotti MT, Mercanti D, Santoni A, Eusebi F. CXC chemokines interleukin-8 (IL-8) and growth-related gene product alpha (GROalpha) modulate Purkinje neuron activity in mouse cerebellum. J Neuroimmunol 1998;92:122–132. [PubMed: 9916887]

Govrin-Lippmann R, Devor M. Ongoing activity in severed nerves: source and variation with time. Brain Res 1978;159:406–410. [PubMed: 215270]

Hargreaves K, Dubner R, Brown F, Flores C, Joris J. A new and sensitive method for measuring thermal nociception in cutaneous hyperalgesia. Pain 1988;32:77–88. [PubMed: 3340425]

Hoch RC, Rodriguez R, Manning T, Bishop M, Mead P, Shoemaker WC, Abraham E. Effects of accidental trauma on cytokine and endotoxin production. Critical Care Medicine 1993;21:839–845. [PubMed: 8504650]

Homma Y, Brull SJ, Zhang J-M. A comparison of chronic pain behavior following local application of tumor necrosis factor alpha to the normal and mechanically compressed lumbar ganglia in the rat. Pain 2002;95:235–246.

Hu P, McLachlan EM. Macrophage and lymphocyte invasion of dorsal root ganglia after peripheral nerve lesions in the rat. Neuroscience 2002;112:23–38. [PubMed: 12044469]

Ignatowski TA, Covey WC, Knight PR, Severin CM, Nickola TJ, Spengler RN. Brain-derived TNFalpha mediates neuropathic pain. Brain Res 1999;841:70–77. [PubMed: 10546989]

Ji RR, Strichartz G. Cell signaling and the genesis of neuropathic pain. Sci STKE 2004;2004:reE14. [PubMed: 15454629]

Kawaguchi S, Yamashita T, Yokogushi K, Murakami T, Ohwada O, Sato N. Immunophenotypic analysis of the inflammatory infiltrates in herniated intervertebral discs. Spine 2001;26:1209–1214. [PubMed: 11389385]

Kawakami M, Tamaki T, Weinstein JN, Hashizume H, Nishi H, Meller ST. Pathomechanism of pain-related behavior produced by allografts of intervertebral disc in the rat. Spine 1996;21:2101–2107. [PubMed: 8893434]

Liu B, Li HQ, Brull SJ, Zhang JM. Increased sensitivity of sensory neurons to tumor necrosis factor alpha in rats with chronic compression of the lumbar ganglia. J Neurophysiol 2002;88:1393–1399. [PubMed: 12205160]

Losy J, Zaremba J, Skrobanski P. CXCL1 (GRO-alpha) chemokine in acute ischaemic stroke patients. Folia Neuropathol 2005;43:97–102. [PubMed: 16012911]

Lu X, Richardson PM. Inflammation near the nerve cell body enhances axonal regeneration. J Neurosci 1991;11:972–978. [PubMed: 1901354]

Lu X, Richardson PM. Responses of macrophages in rat dorsal root ganglia following peripheral nerve injury. Journal of Neurocytology 1993;22:334–341. [PubMed: 8315414]

Martiney JA, Cuff C, Litwak M, Berman J, Brosnan CF. Cytokine-induced inflammation in the central nervous system revisited. Neurochem Res 1998;23:349–359. [PubMed: 9482247]

Milligan ED, Twining C, Chacur M, Biedenkapp J, O'Connor K, Poole S, Tracey K, Martin D, Maier SF, Watkins LR. Spinal glia and proinflammatory cytokines mediate mirror-image neuropathic pain in rats. J Neurosci 2003;23:1026–1040. [PubMed: 12574433]

Morgan R, King D. Shingles: a review of diagnosis and management. Hospital Medicine (London) 1998;59:770–776.

Nakamura M, Ferreira SH. A peripheral sympathetic component in inflammatory hyperalgesia. Eur J Pharmacol 1987;135:145–153. [PubMed: 2884117]

Olmarker K, Myers RR. Pathogenesis of sciatic pain: role of herniated nucleus pulposus and deformation of spinal nerve root and dorsal root ganglion. Pain 1998;78:99–105. [PubMed: 9839819]

Perry VH, Brown MC. Role of macrophages in peripheral nerve degeneration and repair. Bioessays 1992;14:401–406. [PubMed: 1323962]

Poletti CE. Third cervical nerve root and ganglion compression: clinical syndrome, surgical anatomy, and pathological findings. Neurosurgery 1996;39:941–948. 948–949. [PubMed: 8905749]

Qin X, Wan Y, Wang X. CCL2 and CXCL1 trigger calcitonin gene-related peptide release by exciting primary nociceptive neurons. J Neurosci Res 2005;82:51–62. [PubMed: 16047385]

Ramer MS, Murphy PG, Richardson PM, Bisby MA. Spinal nerve lesion-induced mechanoallodynia and adrenergic sprouting in sensory ganglia are attenuated in interleukin-6 knockout mice. Pain 1998;78:115–121. [PubMed: 9839821]

Ramer MS, Thompson SW, McMahon SB. Causes and consequences of sympathetic basket formation in dorsal root ganglia. Pain 1999;(Suppl 6):S111–120. [PubMed: 10491979]

Sato K, Kikuchi S. An anatomic study of foraminal nerve root lesions in the lumbar spine. Spine 1993;18:2246–2251. [PubMed: 8278840]

Satoh K, Konno S, Nishiyama K, Olmarker K, Kikuchi S. Presence and distribution of antigen-antibody complexes in the herniated nucleus pulposus. Spine 1999;24:1980–1984. [PubMed: 10528371]

Schafers M, Lee DH, Brors D, Yaksh TL, Sorkin LS. Increased sensitivity of injured and adjacent uninjured rat primary sensory neurons to exogenous tumor necrosis factor-alpha after spinal nerve ligation. J Neurosci 2003a;23:3028–3038. [PubMed: 12684490]

Schafers M, Svensson CI, Sommer C, Sorkin LS. Tumor necrosis factor-alpha induces mechanical allodynia after spinal nerve ligation by activation of p38 MAPK in primary sensory neurons. J Neurosci 2003b;23:2517–2521. [PubMed: 12684435]

Schon F, Mayer ML, Kelly JS. Pathogenesis of post-herpetic neuralgia. Lancet 1987;2:366–368. [PubMed: 2886824]

Sommer C, Kress M. Recent findings on how proinflammatory cytokines cause pain: peripheral mechanisms in inflammatory and neuropathic hyperalgesia. Neurosci Lett 2004;361:184–187. [PubMed: 15135924]

Sommer C, Marziniak M, Myers RR. The effect of thalidomide treatment on vascular pathology and hyperalgesia caused by chronic constriction injury of rat nerve. Pain 1998a;74:83–91. [PubMed: 9514564]

Sommer C, Schmidt C, George A. Hyperalgesia in experimental neuropathy is dependent on the TNF receptor 1. Exp Neurol 1998b;151:138–142. [PubMed: 9582261]

Song X-J, Hu S-J, Zhang J-M, Greenquist KW, LaMotte RH. Cutaneous hyperalgesia during chronic compression of dorsal root ganglion. Soc Neurosci Abstr 1997;23:497–412.

Song XJ, Hu SJ, Greenquist KW, Zhang J-M, LaMotte RH. Mechanical and thermal hyperalgesia and ectopic neuronal discharge after chronic compression of dorsal root ganglia. J Neurophysiol 1999;82:3347–3358. [PubMed: 10601466]

Song XJ, Zhang JM, Hu SJ, LaMotte RH. Somata of nerve-injured sensory neurons exhibit enhanced responses to inflammatory mediators. Pain 2003;104:701–709. [PubMed: 12927643]

Stoll G, Jander S, Schroeter M. Cytokines in CNS disorders: neurotoxicity versus neuroprotection. J Neural Transm Suppl 2000;59:81–89. [PubMed: 10961421]

Svensson CI, Schafers M, Jones TL, Powell H, Sorkin LS. Spinal blockade of TNF blocks spinal nerve ligation-induced increases in spinal P-p38. Neurosci Lett 2005;379:209–213. [PubMed: 15843065]

Valles A, Grijpink-Ongering L, de Bree FM, Tuinstra T, Ronken E. Differential regulation of the CXCR2 chemokine network in rat brain trauma: Implications for neuroimmune interactions and neuronal survival. Neurobiol Dis 2006;22:312–322. [PubMed: 16472549]

Wagner R, Myers RR. Endoneurial injection of TNF-alpha produces neuropathic pain behaviors. Neuroreport 1996;7:2897–2901. [PubMed: 9116205]

Wall PD, Devor M, Inbal R, Scadding JW, Schonfeld D, Seltzer Z, Tomkiewicz MM. Autotomy following peripheral nerve lesions: experimental anaesthesia dolorosa. Pain 1979;7:103–111. [PubMed: 574931]

Watkins LR, Maier SF. Beyond neurons: Evidence that immune and glial cells contribute to pathological pain states [Review]. Physiological Reviews 2002;82:981–1011. [PubMed: 12270950]

Watkins LR, Maier SF. Immune regulation of central nervous system functions: from sickness responses to pathological pain. J Intern Med 2005;257:139–155. [PubMed: 15656873]

White FA, Sun J, Waters SM, Ma C, Ren D, Ripsch M, Steflik J, Cortright DN, Lamotte RH, Miller RJ. Excitatory monocyte chemoattractant protein-1 signaling is up-regulated in sensory neurons after chronic compression of the dorsal root ganglion. Proc Natl Acad Sci USA 2005;102:14092–14097. [PubMed: 16174730]

Woodham P, Anderson PN, Nadim W, Turmaine M. Satellite cells surrounding axotomised rat dorsal root ganglion cells increase expression of a GFAP-like protein. Neuroscience Letters 1989;98:8–12. [PubMed: 2710403]

Xia M, Hyman BT. GROalpha/KC, a chemokine receptor CXCR2 ligand, can be a potent trigger for neuronal ERK1/2 and PI-3 kinase pathways and for tau hyperphosphorylation-a role in Alzheimer's disease? J Neuroimmunol 2002;122:55–64. [PubMed: 11777543]

Xie W, Strong JA, Meij JT, Zhang JM, Yu L. Neuropathic pain: Early spontaneous afferent activity is the trigger. Pain 2005;116:243–256. [PubMed: 15964687]

Zelenka M, Schafers M, Sommer C. Intraneural injection of interleukin-1beta and tumor necrosis factor-alpha into rat sciatic nerve at physiological doses induces signs of neuropathic pain. Pain 2005;116:257–263. [PubMed: 15964142]

Zhang J-M, Homma Y, Ackerman WE, Brull SJ. Topical application of acidic bupivacaine to the lumbar ganglion induces mechanical hyperalgesia in the rat. Anesthesia & Analgesia 2001;93:466–471. [PubMed: 11473881]

Zhang J-M, Li H, Brull SJ. Perfusion of the mechanically compressed lumbar ganglion with lidocaine reduces mechanical hyperalgesia and allodynia in the rat. J Neurophysiol 2000;84:798–805. [PubMed: 10938306]

Zhang J-M, Li H, Munir MA. Decreasing sprouting of noradrenergic sympathetic fibers in pathologic sensory ganglia: new mechanism and approach for treating neuropathic pain using local anesthetics. Pain 2004;109:143–149. [PubMed: 15082136]

Zhang J-M, Li HQ, Liu B, Brull SJ. Acute topical application of tumor necrosis factor alpha evokes protein kinase A-dependent responses in rat sensory neurons. J Neurophysiol 2002;88:1387–1392. [PubMed: 12205159]

Zhang J-M, Song XJ, LaMotte RH. An in vitro study of ectopic discharge generation and adrenergic sensitivity in the intact, nerve-injured rat dorsal root ganglion. Pain 1997;72:51–57. [PubMed: 9272787]

Zhang J-M, Song XJ, LaMotte RH. Enhanced excitability of sensory neurons in rats with cutaneous hyperalgesia produced by chronic compression of the dorsal root ganglion. J Neurophysiol 1999;82:3359–3366. [PubMed: 10601467]

Zhou XF, Deng YS, Chie E, Xue Q, Zhong JH, McLachlan EM, Rush RA, Xian CJ. Satellite-cell-derived nerve growth factor and neurotrophin-3 are involved in noradrenergic sprouting in the dorsal root ganglia following peripheral nerve injury in the rat. European Journal of Neuroscience 1999;11:1711–1722. [PubMed: 10215925]

Figure 1.

Inflaming the L5 DRG with zymosan/IFA induced prolonged bilateral mechanical hyperalgesia and allodynia. **A, B.** Changes in the withdrawal threshold to mechanical indentation of the hind paws in rats receiving local deposition of zymosan of 1 μg (low dose; **A**) or 10 μg (high dose; **B**) in IFA. Mean withdrawal thresholds to mechanical indentation are plotted as a function of postoperative time. Each data point is the mean threshold changes obtained on each day of testing. “Day 0” represents the withdrawal threshold changes averaged from 3 preoperative testing sessions (one session every 3 days). One-way RM ANOVA: Low-dose group, significant decreases from preoperative level (*$p<0.05$) beginning on the first postoperative day in the ipsilateral foot and on the third postoperative day in the contralateral side. High-dose group, significant decreases (*$p<0.05$) beginning on the first postoperative day in both the ipsilateral and contralateral foot. **C.** Control rats receiving local injection of buffered saline. **D:** Incidence of foot withdrawal response to light stroke of the ventral surface using a piece of cotton swab.

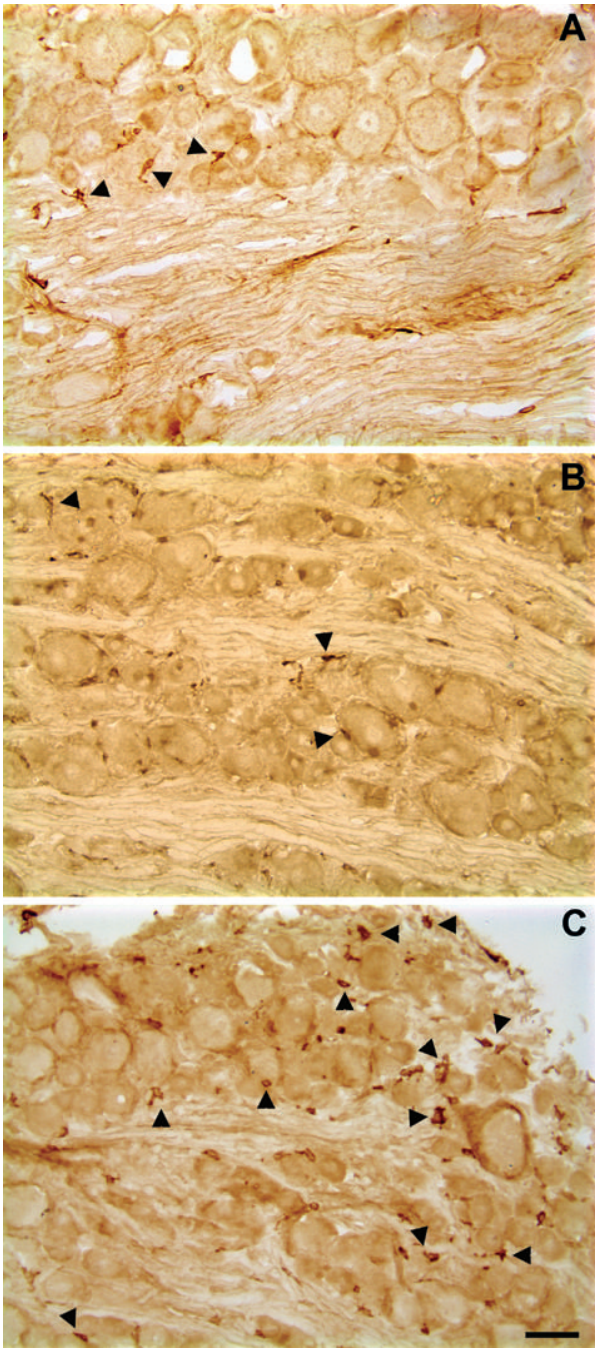

Figure 2.

Light microscopic images of macrophage responses in zymosan-treated (10 μg) lumbar ganglia. Immunohistochemistry with ED-2 antibody on frozen sections (10 μm thick) of normal and zymosan-treated DRGs on POD 3. **A**: Example of a section from normal DRG with a few macrophages (arrow); **B**: representative example of an image from sham DRG on POD 3. **C.** DRG with immunological activation by injection (10 μg in IFA) of zymosan 3 days prior to immunostaining. Scale bar=50 μm.

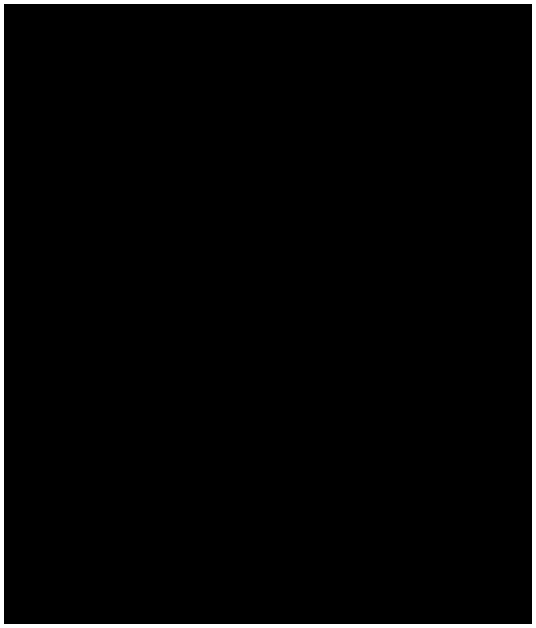

Figure 3.

Zymosan treatment (10 μg in IFA) induces prolonged macrophage response in the ipsilateral and, to a lesser degree, the contralateral DRGs. Top: Comparison of macrophage densities in the L5 DRGs subjected to various treatments. Immunohistochemistry with ED-2 antibody was performed in normal, sham, and Zymosan/IFA-treated DRG sections on postoperative day 3. Each data point is the mean density obtained from 8–10 sections of 3 ganglia from 3 rats. *P<0.05, Student's t-test compared to normal. ##P<0.01, Student's t-test compared to sham group. Bottom: Time course of macrophage response in the DRGs after zymosan/IFA deposit. *P<0.05, Student's t-test compared to day "0"; **P<0.01, Student's t-test compared to day "0".

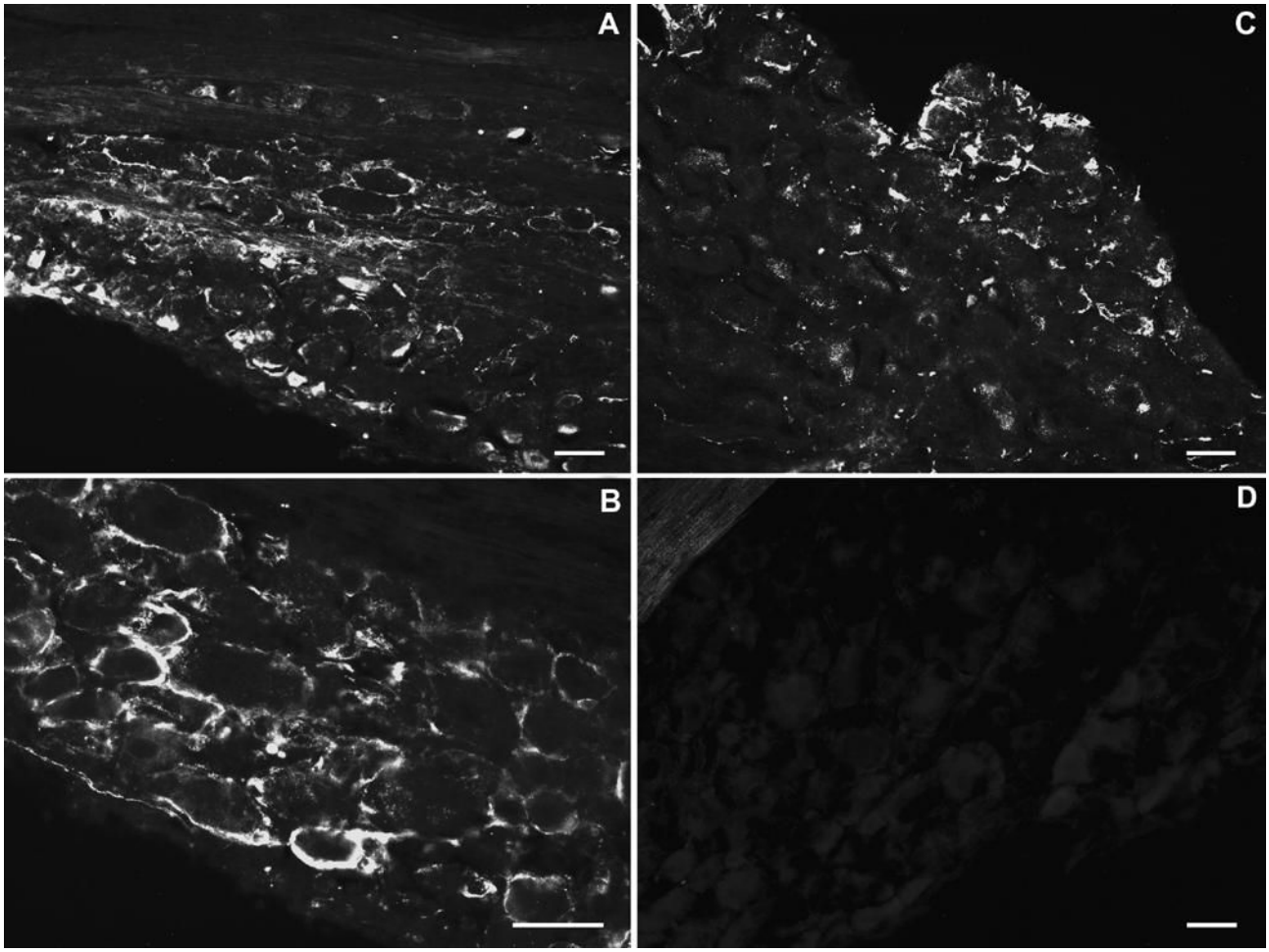

Figure 4.

Light microscopic images of satellite glial activation (GFAP-positive) in zymosan/IFA-treated lumbar ganglia. Immunohistochemistry with anti- GFAP antibody was performed on frozen sections (10 μm thick) of normal and zymosan/IFA-treated DRGs on POD 3. **A, B:** L4 DRG ipsilateral to zymosan/IFA injection; **C:** L4 DRG contralateral to zymosan/IFA injection; **D:** normal, untreated DRG. Scale bar = 50 μm.

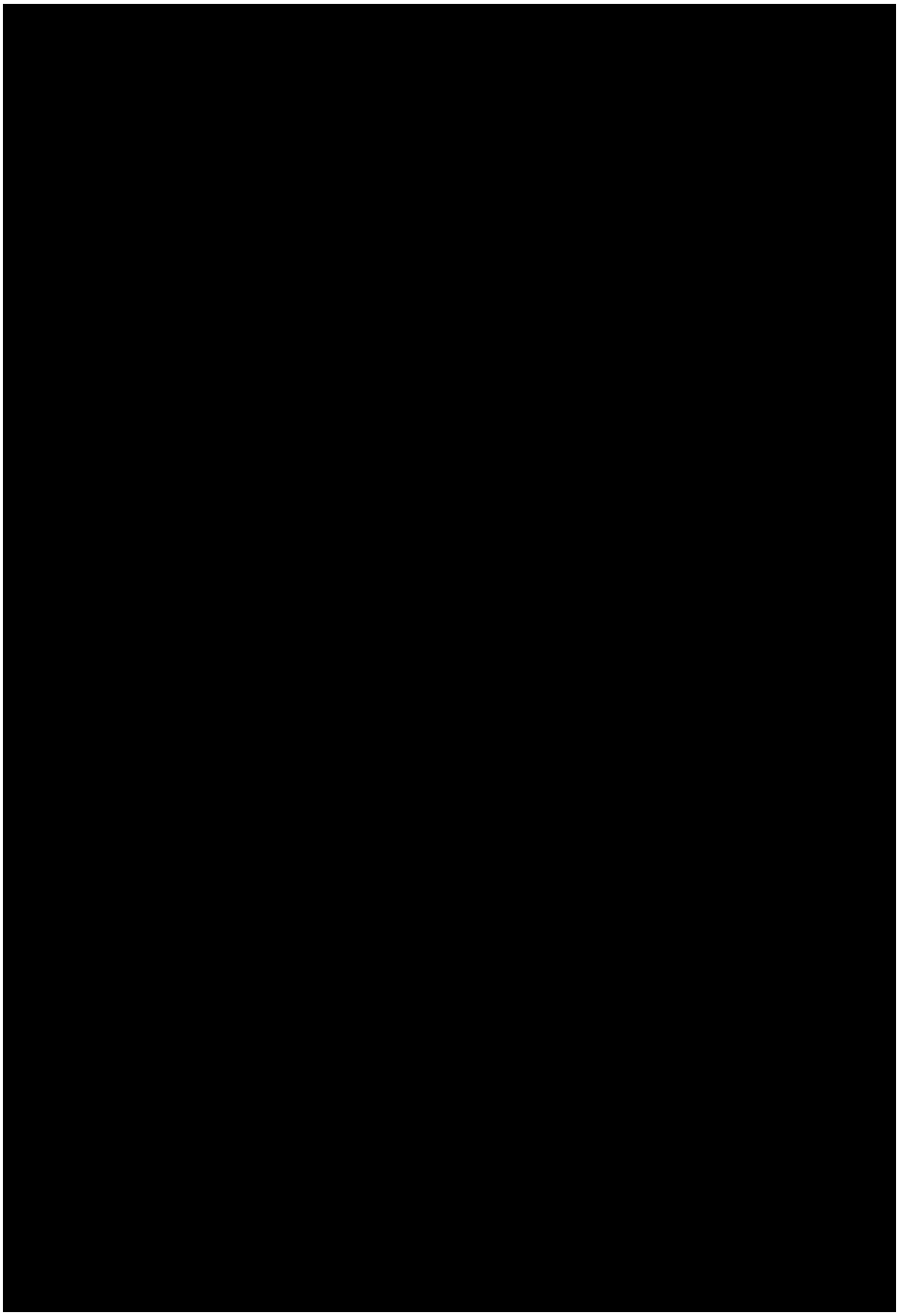

Figure 5.
Selective up-regulation of cytokines in the inflamed DRGs. Time course of levels of the indicated cytokines is shown on the left; the normal values in unoperated rats are indicated by the dotted lines. Fractional changes (normal rat values used as the basis) are shown on the right. Zymosan dose was 10 μg.

Figure 6.
Selective down-regulation of cytokines in the inflamed DRGs. Time course of levels of the indicated cytokines is shown on the left; the normal values in unoperated rats are indicated by the dotted lines. Fractional changes (normal rat values used as the basis) are shown on the right. Zymosan dose was 10 μg.

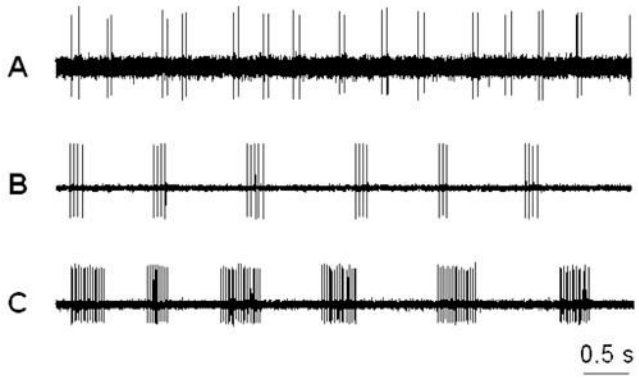

Figure 7.
Three typical patterns of bursting discharge recorded from dorsal root fibers (Aβ) of the DRGs inflamed with Zymosan (10 μg). A: doublet discharges; B: short-bursting regular discharges; C: long-bursting discharges. The majority of spontaneously active neurons exhibited a short-bursting pattern.

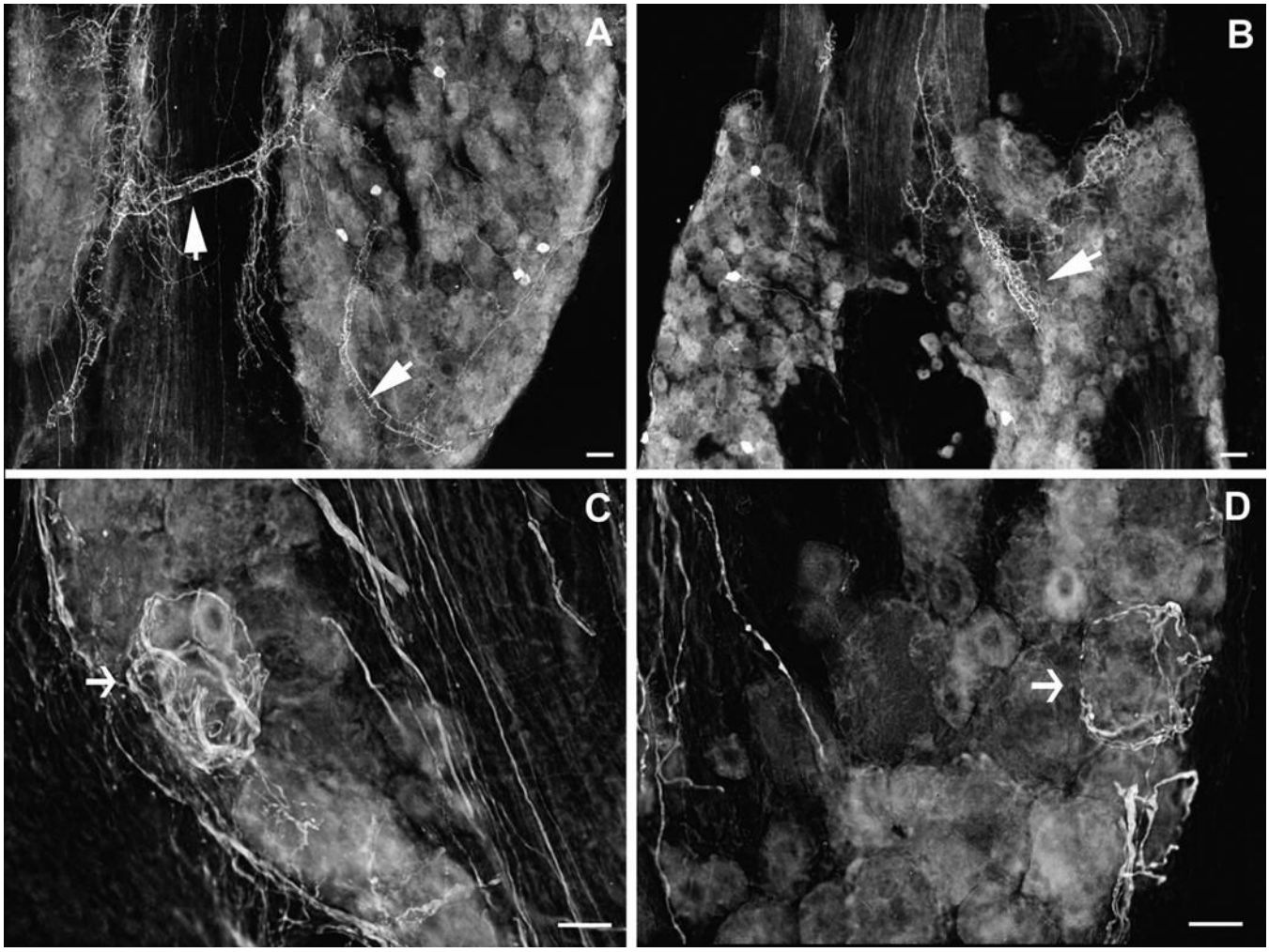

Figure 8.
Light microscopic photo images of the sprouted sympathetic fibers in the lumbar ganglia following localized inflammatory irritation with 10 μg Zymosan in IFA on postoperative day 7. A, B: TH-ir sympathetic fibers sprout from the vascular processes. C, D: sprouted fibers form basket structures around large DRG neurons. Images are inverted from the originals. Scale bar =50 μm.

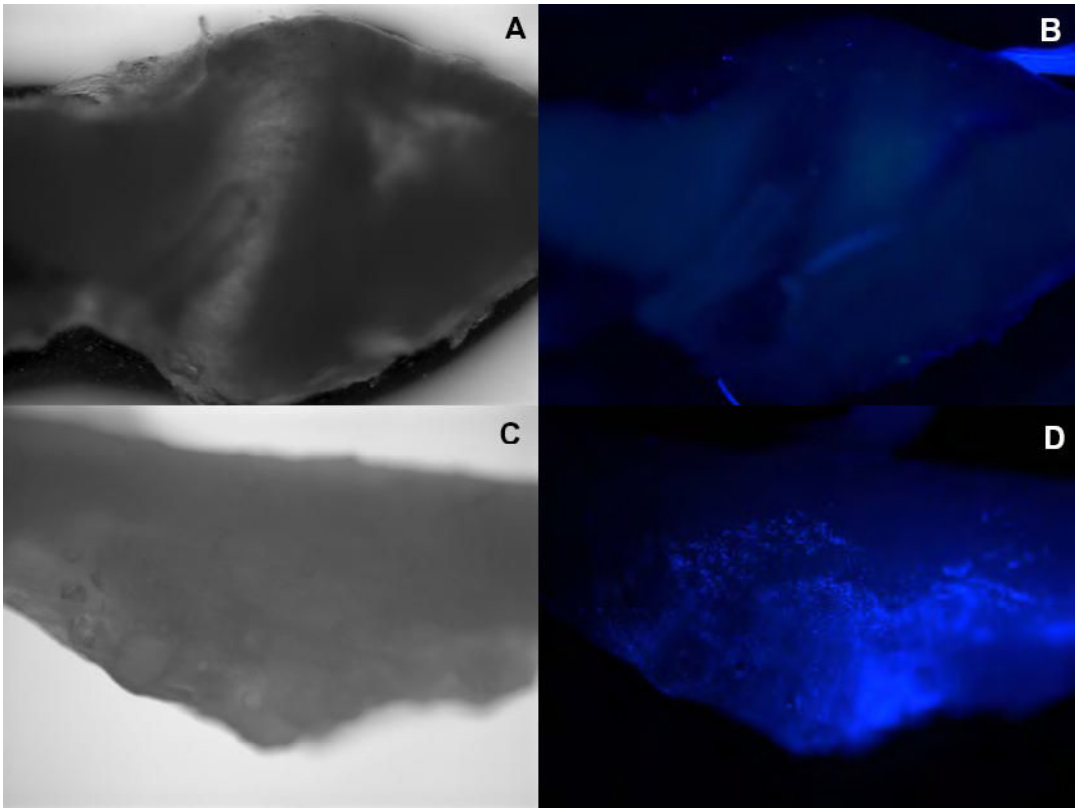

Top (A, B): Contralateral L5 DRG
Bottom (C, D): Ipsilateral L5 DRG
Scale: 4x
Note that the ipsilateral L5 DRG is covered by the fluospheres (bright spots).

Table 1

Cytokine concentrations in normal, sham operated, zymosan/IFA-inflamed (10 μg), and contralateral DRGs measured on postoperative day 3. Concentrations of cytokines are given as mean ± S.E.M. in units of per mg of tissue (Part A) as well as per mg protein (Part B)

Part A

Cytokine	Concentration (pg/mg tissue)				Fold Change Ipsi vs.Normal	Fold Change Ipsi vs.Sham	Estimated Detection Limit (pg/mg)
	Normal	Sham	LID Ipsi	LID Cont			
GM-CSF	-	-	-	-	-	-	0.009 (0.64 pM)
GRO/KC	0.52±0.09	1.02 ±0.34	3.87 ±0.85#	3.04 ±0.88#	9.68$	6.89#	0.014 (1.86 pM)
IFN	0.63±0.20	1.06 ±0.60	0.57 ±0.18	0.47±0.21	0.90	0.69	0.034 (2.20 pM)
IL-10	-	-	-	-	-	-	0.027 (1.42 pM)
IL-12	0.18±0.05	0.14 ±0.04	0.11 ±0.01	0.08±0.04	0.60*	0.95	0.029 (0.41 pM)
IL-18	4.8±1.0	4.7±0.4	8.4±1.6	5.53±0.90	1.75*	1.78	0.034 (1.40 pM)
IL-1α	0.47±0.10	0.37 ±0.02	0.61 ±0.17	0.57±0.46	1.29	1.94	0.044 (2.48 pM)
IL-1β	0.45±0.13	0.42 ±0.13	0.93 ±0.13*	1.08±0.66	2.09#	2.74	0.016 (0.94 pM)
IL-2	0.59±0.06	0.46 ±0.14	0.27 ±0.04#	0.29 ±0.11*	0.46#	0.79	0.026 (1.69 pM)
IL-4	0.05±0.01	-	-	0.01 ±0.00*	⇓	⇓	0.016 (1.16 pM)
IL-5	-	-	-	-	-	-	0.020 (1.45 pM)
IL-6	0.36±0.07	1.05 ±0.43	2.49 ±0.65*	1.94 ±0.75*	7.00*	3.04	0.069 (3.18 pM)
MCP-1	0.70±0.10	1±0.18*	1.80±0#	1.11±0.22	2.56$	1.82	0.027 (1.91 pM)
TNF-α	0.42±0.12	0.56 ±0.29	0.26 ±0.10	0.33±0.04	0.63	0.61	0.031 (1.84 pM)

Part B

Cytokine	Concentration (pg/mg tissue)				Fold Change Ipsi vs. Normal	Fold Change Ipsi vs. Sham	Estimated Detection Limit (pg/mg)
	Normal	Sham	LID Ipsi	LID Cont			
GM-CSF	-	-	-	-	-	-	0.21
GRO/KC	17.0±3.9	23.9±8.1	92.4±25.9*	55.8±17.0*	5.4$	3.8$	0.33
IFN	19.0±4.8	24.9±15.5	11.0±3.8	8.9±4.3	0.6	0.5	0.77
IL-10	-	-	-	-	-	-	0.60
IL-12	5.3±1.3	3.3±0.7	2.5±0.2	1.6±0.9	0.5$	0.8*	0.65
IL-18	147±30	117±22	231±76	98.7±12.0	1.6	2.0	0.76
IL-1α	14.0±2.4	9.3±1.7	15.0±4.6	9.6±7.4	1.1	1.7	0.99
IL-1β	13.6±4.0	10.4±3.6	22.9±5.9	18.7±10.5	1.7#	2.2	0.37
IL-2	19.1±3.1	11.2±3.7	6.5±1.1#	5.6±2.5*	0.3#	0.5	0.58
IL-4	1.8±0.5	-	-	0.2±0.1	⇓	⇓	0.36
IL-5	-	-	-	-	-	-	0.46
IL-6	11.0±1.9	25.4±11.1	53.5±11.1#	36.6±15.7	4.9*	2.1	1.55
MCP-1	22±2.9	31±8.5	47.2±14	20.1±4.3	2.2	1.6	0.60
TNF-α	12.9±3.1	13.3±7.5	5.6±1.8	6.0±0.6	0.4*	0.4	0.70

Significance of concentrations changes vs. normal is indicated by * ($p<0.05$), # ($p<0.01$), and $ ($p < 0.001$), based on Student's t-test. Significance of fold increases or decreases for LID compared to normal (5^{th} column) and to sham (6^{th} column) are indicated by the same symbols, and were obtained by ratio t-tests (on the logs of the values). Cells filled by "–" indicate experiments for which a value could not be obtained because at least some of the experimental values were lower than the detection unit. The ⇓ symbol indicates that the nominal average value, including as zeroes those experiments with values below the detection level, suggested that the fold increase was <1. N = 3 experiments for the sham and contralateral values, and 5 for the normal and LID values; each experimental measurement was on samples containing 4 ganglia combined from 2 rats, measured in duplicate. The estimated detection limits were obtained by normalizing the lowest detectable cytokine concentration (as specified by the kit manufacturer) by the average experimental tissue weight (Part A) or average experimental protein weight (Part B), for each experiment. Conversion of detection limits from pg/mg tissue to pM was done by assuming 1mg tissue was predominantly water and hence had a volume of 1 μL. Ipsi: ipsilateral; Cont: contralateral.

Table 2

Incidence of spontaneous activity of DRG neurons recorded from dorsal root C, Aδ, and Aβ fibers of normal and LID rats.

	Normal (n=5)			POD3 (n=4)				POD7 (n=7)				POD14 (n=6)		
	SA	**Total**	**%**	**SA**	**Total**	**%**	***p***	**SA**	**Total**	**%**	***p***	**SA**	**Total**	**%**
C	0	71	0	8	74	10.8	*0.049*	6	72	8.3	*0.085*	3	81	3.7
Aδ	1	58	1.7	9	105	8.6	*0.282*	5	56	8.9	*0.229*	5	94	5.3
Aβ	8	538	1.5	83	628	13.2	$<10^{-4}$	52	320	16	$<10^{-4}$	70	685	10.2
Total	9	667	1.3	100	807	12.4	$<10^{-4}$	63	448	14	$<10^{-4}$	78	860	9.1

SA: number of spontaneously active fiber

Total: total number of activating fibers

%: incidence of spontaneous activity.

p: p value (vs. Normal), Fishers exact test.